Confinement of spin-orbit induced Dirac states in quantum point contacts

Tommy Li
School of Physics, University of New South Wales, Sydney 2052, Australia
(Received 2 February 2015; published 10 August 2015)

The quantum transmission problem for a particle moving in a quantum point contact in the presence of a Rashba spin-orbit interaction and applied magnetic field is solved semiclassically. A strong Rashba interaction and parallel magnetic field form emergent Dirac states at the center of the constriction, leading to the appearance of resonances which carry spin current and become bound at high magnetic fields. These states can be controlled *in situ* by modulation of external electric and magnetic fields, and can be used to turn the channel into a spin pump which operates at zero bias. It is shown that this effect is currently experimentally accessible in p-type quantum point contacts.

DOI: 10.1103/PhysRevB.92.085302 PACS number(s): 73.23.Ad, 72.25.Dc, 73.63.Nm

One-dimensional (1D) spin-orbit coupled systems have recently attracted significant interest in the context of quantum information and spintronics, playing a key role in the search for emergent Majorana fermions [1–3] and the generation of spin-polarized current [4–9]. Interest in these systems has sparked several theoretical studies of their modified conductance properties [10–18]. In this work I present a semiclassical solution to the scattering problem for a quantum point contact (QPC) in the presence of the Rashba spin-orbit interaction and a parallel magnetic field. The quantum states near the center of the constriction are described by a one-dimensional massive Dirac equation, with the Rashba constant and magnetic field playing the roles of the speed of light and Dirac mass, respectively. The emergent fermion and antifermion states behave differently in the channel, with the latter falling into the center of the constriction, forming resonant states. This process may be considered a manifestation of Schwinger pair production, an effect which is well known in high-energy physics [19–21] and has recently been investigated in the context of emergent two-dimensional Dirac systems [22,23]. When the applied magnetic field is strong, the resonances become bound and generate a concentration of spin current in the channel. The properties of these states are highly sensitive to the strength of the spin-orbit interaction and the applied magnetic field, implying that they can be controlled *in situ* by modulation of external fields. These results suggest an experiment in which repeated capture and release of particles inside the channel leads to a net spin polarization in the leads, transforming the channel into a spin pump and an injector of spin current which operates in the absence of a source-drain bias. While this effect exists in principle for both n and p type systems, consideration of experimental parameters for existing systems suggests that hole quantum point contacts provide an ideal candidate for the realization of this effect.

I consider a QPC defined by lateral patterning in a semiconductor heterostructure, which is described by the two-dimensional Hamiltonian

$$H_{2D} = \frac{p_x^2 + p_y^2}{2m} + \phi(x,y) + H_{so} + H_Z,$$
$$\phi(x,y) = \frac{m\omega_y^2 y^2}{2} - \frac{m\omega_x^2 x^2}{2}, \tag{1}$$

where m is the effective mass and the electrostatic potential in the heterostructure plane $\phi(x,y)$ is modeled as a saddle point parametrized by frequencies ω_x,ω_y in directions parallel (x) and perpendicular (y) to the QPC [24]. I assume the presence of both spin-orbit coupling H_{so} and Zeeman interaction H_Z. To leading order the Hamiltonian (1) generates one-dimensional scattering states (in the x direction) which are harmonically confined in the y direction. The wave function takes the form

$$\psi(x,y) = \psi_{1D}(x)\varphi_n(y),$$
$$\left[\frac{p_y^2}{2m} + \frac{m\omega_y^2 y^2}{2}\right]\varphi_n(y) = \hbar\omega_y\left(n + \frac{1}{2}\right)\varphi_n(y). \tag{2}$$

I consider the Rashba interaction, which is known to be strong in narrow-gap n-type systems [25–27]; the spin-orbit interaction in this case has the form $H_{so} = \alpha(p_x\sigma_y - p_y\sigma_x)$ [28], where α is the Rashba constant. Our starting point for determining the effect of the spin-dependent terms on transmission through the contact is the 1D Hamiltonian which acts on the scattering wave function $\psi_{1D}(x)$. Projecting the Hamiltonian onto transverse states, we obtain

$$H_n = \frac{p_x^2}{2m} - \alpha p_x\sigma_y - \beta\sigma_x + U_n(x),$$
$$U_n(x) = \hbar\omega_y\left(n + \frac{1}{2}\right) - \frac{m\omega_x^2 x^2}{2}, \tag{3}$$

where $\beta = \frac{1}{2}g\mu_B B_x$ and g is the g factor. Note that in the Rashba interaction we replace p_y with its expectation value $\langle\phi_n|p_y|\phi_n\rangle = 0$, since the operator only couples different transverse levels. Coupling between different transverse channels may be accounted for in perturbation theory; one then finds to all orders that the spin-dependent terms in the Hamiltonian (3) are unchanged except for a renormalization of coefficients, although additional spin-independent terms will appear at higher order in p_x.

In the case of p-type systems, the Rashba interaction is strong even in larger gap materials (such as GaAs) due to valence band mixing [29,30]. The spin-dependent terms take the form [31]

$$H_{so} = \frac{i\alpha'}{2}(p_+^3\sigma_- - p_-^3\sigma_+),$$
$$H_Z = -\kappa\mu_B(B_+ p_+^2\sigma_- + B_- p_-^2\sigma_+), \tag{4}$$

where $p_+ = p_x + ip_y$, etc. Taking the projection onto harmonic oscillator levels gives the same Hamiltonian (3) with $\alpha = 3\alpha'\langle\varphi_n|p_y^2|\varphi_n\rangle$, $\beta = -\kappa\langle\varphi_n|p_y^2|\varphi_n\rangle$, with the exception of additional terms quadratic and cubic in the momentum,

$$\delta H_{1D} = -2\kappa\mu_B B_x p_x^2\sigma_x + \alpha' p_x^3\sigma_y. \quad (5)$$

As in the case of the n-type Rashba interaction, accounting for coupling between different oscillator levels $\varphi_n(y)$ in perturbation theory does not alter the Hamiltonian (3) to quadratic order in momentum, except for a renormalization of parameters. Hereafter I consider scattering within a single transverse channel and refer to the 1D barrier as $U_n(x) = U(x)$ and its maximum as $U(x = 0) = U_0$.

The scattering wave function is formed in a region inside the constriction where the kinetic energy is heavily suppressed by the barrier potential $U(x)$. At the semiclassical turning points, $p_x \to 0$, terms of higher order in momentum become irrelevant, and we may therefore consider the terms (3) which are common to both electron and hole systems. The dispersion corresponding to the momentum-dependent terms in Eq. (3) consists of spin-split bands $\epsilon_k^{\pm}$ given by

$$\epsilon_k^{\pm} = \frac{\hbar^2k^2}{2m} \pm \sqrt{\alpha^2\hbar^2k^2 + \beta^2}. \quad (6)$$

For magnetic fields below a critical value $\beta < \beta_c = m\alpha^2$, the lower band has a "Mexican hat" shape, with a local maximum at $k = 0$; the dispersion in this case is shown in Fig. 1(a). Note that the shape of the upper and lower branches near $k = 0$ is governed by an anticrossing created by the combination of the Rashba interaction and a Zeeman interaction $0 < \beta < \beta_c$.

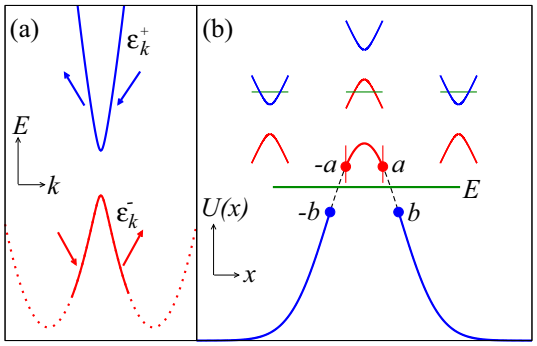

FIG. 1. (Color online) Confinement of a Dirac fermion in a QPC, which occurs when the parallel magnetic field is below the critical value $\beta = \frac{1}{2}g\mu_B B_x < \beta_c$. (a) The 1D dispersion near the anticrossing, with the bold lines showing the region in which Dirac fermion behavior is expected to appear. The two spin branches ϵ_k^+,ϵ_k^- are identified as the positive and negative energy Dirac states, respectively. Arrows indicate the direction of spin polarization. (b) The potential barrier $U(x)$ (lower curve), and the situation in momentum space (three upper figures). There are three regions which form the scattering wave function. In the asymptotic region $|x| > b$, the kinetic energy lies in the upper (positive energy) branch. Inside the barrier, $|x| < a$, the kinetic energy lies in the lower (negative energy) branch. Quantization of motion in the region bounded by vertical lines gives rise to a subbarrier resonance. The energy is indicated by the horizontal line. The tunneling regions are shown with dashed lines.

For incident energies tuned close to the top of the barrier, dynamics in the scattering region are dominated by the linear-in-momentum term in Eq. (3); to leading order in p_x we obtain the Dirac equation

$$[-\alpha p_x\sigma_y - \beta\sigma_x + U(x)]\psi(x) = E\psi(x). \quad (7)$$

We may identify the upper and lower branches of the dispersion ϵ_k^+,ϵ_k^- near the anticrossing with the *positive energy* and *negative energy* Dirac states, respectively. Note that the parallel magnetic field creates a tunable Dirac gap of energy 2β.

Transmission through the constriction differs qualitatively in the situations $\beta > \beta_c$ and $\beta < \beta_c$. In the former, the transmission probability in each band simply drops to zero as the Fermi energy successively crosses the bottom of each spin-split band, leading to the appearance of plateaus at $G = (n + \frac{1}{2})\frac{2e^2}{h}$ in the channel conductance which is the experimental signature of Zeeman-split subbands [32]. The second situation, $\beta < \beta_c$, is highly non-trivial due to the possibility of tunneling from a positive to a negative energy state when the barrier is sufficiently high, $U_0 > E + \beta$. Tunneling occurs at the sides of the potential barrier [indicated by dashed lines in Fig. 1(b)] in the regions where the kinetic energy lies within the Dirac gap. The result is the appearance of a particle in a negative energy state at the top of the barrier, which is characterized by a negative effective mass, $\frac{1}{m^*} = \frac{1}{m}(1 - \frac{m\alpha^2}{\beta}) < 0$ (or equivalently, positive effective mass but opposite electric charge) and therefore sees the repulsive potential as a quantum well. This shows that there exist two types of charge carriers in the channel, which exhibit qualitatively different behavior in the electrostatic potential $U(x)$: the positive energy states in the branch ϵ_k^+ fall away from the barrier, while the states in the *antifermion* branch ϵ_k^- fall towards the barrier. This process is illustrated in Fig. 1(b). The lower curve shows the potential $U(x)$, with the tunneling region shown with dashed lines. The scattering wave function is formed by two pairs of turning points $x = \pm b$ (assuming a symmetric barrier) and $x = \pm a$. The situation in momentum space is shown in the three figures in the upper part of the same panel. In the regions $|x| > b$, the kinetic energy (shown with a horizontal line) lies in the upper branch, and the particle accelerates away from the barrier. In the region $|x| < a$, the kinetic energy lies in the lower branch. In this region the particle behaves as an antifermion; it falls into the barrier and becomes confined. Quantization of motion between the turning points $x = \pm a$ gives rise to a resonant state; the energy of the resonant state is shown by the horizontal line intersecting the lower curve in Fig. 1(b). Note that the kinetic energy of the "antifermion" must remain above the bottom of the lower branch $E_{\min}$ in order for free motion to persist in the confinement region; the particle is expected to behave as a Dirac fermion when $E - U(x) > E_{\min}$. The range of energies in which resonances are expected to exist is given by

$$E + |E_{\min}| > U_0 > E + \beta, \quad E_{\min} = -\frac{m\alpha^2}{2} - \frac{\beta^2}{2m\alpha^2}; \quad (8)$$

this condition also implies that resonances will appear on conductance plateaus on which only one spin band is fully transmitted.

The existence of two species of carriers which accelerate in opposite directions in the same electric field may be regarded as a manifestation of Schwinger's mechanism for the spontaneous generation of fermion-antifermion pairs in strong electric fields [19]. While ubiquitous in quantum electrodynamics [20,21], direct observation of pair production requires electric fields $eE > \frac{m^2c^3}{\hbar} \gtrsim 10^{16}$ V cm^{-1} which to date have only been accessible in high-energy collisions [33]. In the condensed matter context, this effect has been studied theoretically in graphene [22,23] and is closely related to the phenomenon of atomic collapse recently observed in the material [34]. In our case, the Schwinger mechanism distinguishes the localized "Dirac" state from quasibound states arising from double barriers, edge or multichannel effects as previously studied [14,16–18], and as we shall see later, gives them properties which will enable them to facilitate pumping of spin across the channel.

The transmission probability for a state incident in the upper branch ϵ_k^+ may be derived by consideration of the explicit structure of the scattering wave function. The wave function consists of an asymptotic wave with positive energy which undergoes reflection at the sides of the barrier, $x = \pm b$, and a negative energy part corresponding to free motion inside the barrier, $|x| < a$. The positive energy and negative energy components of the wave function are coupled by tunneling in the regions $a < |x| < b$, leading to a finite lifetime which is proportional to the inverse tunneling rate. Approximating the barrier by a linear function, $U'(x) = \lambda$, the resonant width is given by $\tau^{-1} \propto e^{-2\pi\gamma}$, where the exponent γ is given by Schwinger's formula [19] upon identification of β with the rest energy and α with the effective speed of light:

$$\gamma = \frac{\beta^2}{2\alpha\lambda\hbar}. \tag{9}$$

Accounting for periodic motion in the confinement region $|x| < a$ and tunneling, we obtain explicitly for the transmission probability

$$T = \left| \frac{1}{e^{2\pi\gamma} + (e^{2\pi\gamma} - 1)e^{i\oint kdx + i\delta\varphi}} \right|^2, \tag{10}$$

where $\oint kdx$ is the semiclassical phase acquired by the "antifermion" over one period of semiclassical motion. In the tunneling regions, the solution of the Dirac equation (7) may be expressed analytically in terms of the parabolic cylinder functions, which leads to a phase shift $\delta\varphi = 2\mathrm{Arg}\Gamma(i\gamma) - 4\gamma[\ln 2\sqrt{\gamma} - 1] + \frac{\pi}{2}$. This phase shift appears in the WKB quantization condition for the existence of a standing wave, $\oint kdx = 2\pi(n + \frac{1}{2} - \delta\varphi)$ at energies corresponding to the location of the Breit-Wigner resonances. We may regard (10) as the general semiclassical expression for the transmission probability of a one-dimensional massive Dirac fermion in a smooth potential barrier. In the limit of strong magnetic fields $\beta \gg \sqrt{\alpha\hbar\lambda}$, the resonant states become bound. In the opposite limit $\gamma \to 0$, resonant tunneling occurs over a broad range of energies, reflecting the Klein paradox for ultrarelativistic Dirac fermions [35,36]. Note that we have considered a state with asymptotic energy in the upper branch, ϵ_k^+; in the semiclassical approximation a particle incident from the lower branch ϵ_k^- does not undergo reflection at energies within the Dirac gap and the corresponding transmission probability is nonresonant.

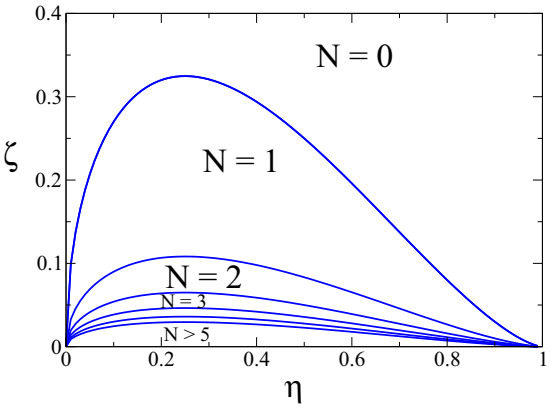

FIG. 2. (Color online) Predicted number of quasibound states for parameters η, ζ, given by Eq. (12).

Approximating the QPC potential as a parabolic barrier, $U(x) \approx U_0 - \frac{m\omega_x^2 x^2}{2}$, the resonant spectrum is equivalent (upon reversing the sign of the energy) to that of a harmonic oscillator with mass $|m^*|$ and oscillator frequency $\omega^* = \sqrt{|\frac{m}{m^*}|}\omega_x$,

$$E_n = U_0 - \beta - \omega^*\left(n + \tfrac{1}{2}\right). \tag{11}$$

The $n = 0$ mode possesses the highest energy, with higher modes forming an inverted tower of oscillator states extending downward in energy. In deriving the spectrum (11) I assume that the lower band may be approximated by a quadratic dispersion $\epsilon_k^- \approx -\beta + \frac{\hbar^2k^2}{2m^*}$, so that in the semiclassical picture the resonant states correspond to simple harmonic motion confined between two turning points $x = \pm a$. (In this limit we also have $\delta\varphi \to 0$.) The spectrum terminates at finite n due to the condition (8). This condition may be expressed in terms of parameters $\zeta = \frac{\omega}{m\alpha^2}$, $\eta = \frac{\beta}{m\alpha^2}$ as

$$\zeta < \frac{1}{2n+1}(1-\eta)^{\frac{3}{2}}\eta^{\frac{1}{2}}. \tag{12}$$

The number of quasibound states predicted by (12) in different regions of the space of parameters (η, ζ) is shown in Fig. 2. In order to observe resonances we require the variation of the potential inside the channel to be smooth compared to the energy scale of the spin-orbit interaction, $\zeta \ll 1$. The optimal regime, in which a large number of particles is trapped in the constriction, occurs when $\eta \approx \frac{1}{4}$. Note that the number of quasibound states is much less sensitive to the size of the magnetic field than to the shape of the confining potential.

Let us now address the possibility of observing resonant Dirac states in the typical experimental situation. Near pinch-off, the barrier height is tuned to the Fermi energy, $U_0 \approx E_F$. We may parametrize the barrier in terms of the QPC length, $U_0 = \frac{1}{2}m\omega^2(\frac{l}{2})^2$, to obtain

$$\zeta = \frac{2}{k_F l}\left(\frac{\hbar k_F}{m\alpha}\right)^2. \tag{13}$$

The value of l is limited by the ballistic mean free path, which is approximately 1 μm in 2D GaAs. Taking $l = 1$ μm,

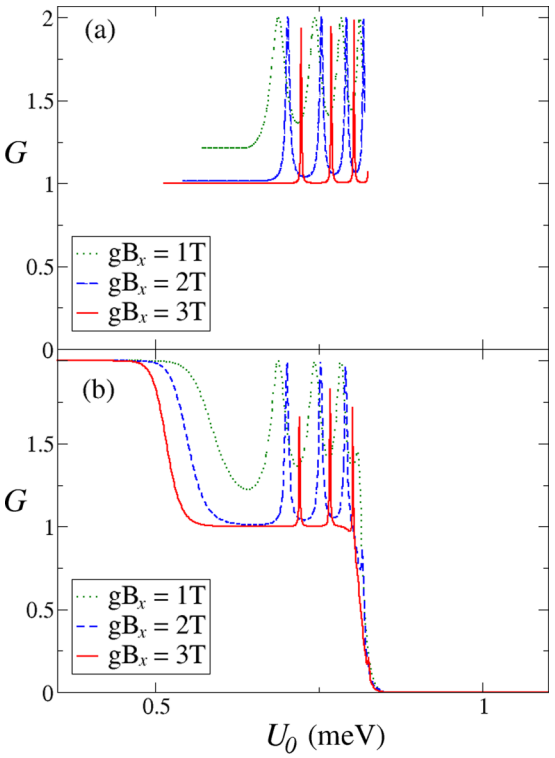

FIG. 3. (Color online) The QPC conductance in units of $\frac{e^2}{h}$ for a Gaussian barrier $U(x) = U_0 e^{-\frac{x^2}{w^2}}$ with parameters $w = 50$ nm, $E_F = 0.6$ meV, $\frac{m\alpha}{\hbar k_F} = 0.6$, and values of magnetic field $gB_x = 3$ T (solid, red), 2 T (dashed, blue), 1 T (dotted, green). (a) The conductance obtained from the analytical formula for the resonant transmission probability (10). (b) The conductance obtained by brute-force numerical integration of the Schrödinger equation corresponding to the Hamiltonian (3).

at typical experimental density $n = 10^{11}$ cm^{-2} in the 2D regions, we have $k_F l \approx 10^2$; in the strongly spin-orbit coupled materials InSb and InAs, the conduction band effective mass ($m \approx 10^{-2} m_e$) is prohibitively small despite the strong Rashba effect, since $\frac{\hbar k_F}{m\alpha} \approx 10^2$ at typical electric fields $\alpha \propto E_z = 10^6$ V m^{-1}. While in principle the 1D band mass may be renormalized by inter-subband coupling, the initial value $\zeta \sim 10^2$ would require a renormalization by more than two orders of magnitude. In p-type point contacts, the larger value of m leads to a stronger spin-orbit interaction as a proportion of the Fermi energy. The coefficient of the 1D Rashba interaction α may be determined by magnetotransport studies in 2D hole systems; we obtain $0.6 \leqslant \frac{m\alpha}{\hbar k_F} \leqslant 1$ from such studies in GaAs-AlGaAs heterojunctions [29,30]. Taking typical values [37] for the hole density $n = 10^{11}$ cm^{-2} and $m = 0.4 m_e$, we obtain $\eta = \frac{1}{5}$, $\zeta = \frac{1}{18}$ at $gB_x = 3$ T for the lower value $m\alpha = 0.6\hbar k_F$. In this regime (12) predicts $N = 3$.

The QPC conductance corresponding to the classical transmission probability (10) is shown in Fig. 3(a) for a Gaussian barrier $U(x) = U_0 e^{-\frac{x^2}{w^2}}$ with parameters $\frac{m\alpha}{\hbar k_F} = 0.6$, $w = 0.5$ μm and magnetic field $gB_x = 1$ T, 2 T, 3 T (for hole QPCs the typical value is $g = 0.5$ [38]). The conductance is shown on the plateau $E - \beta < U_0 < E - E_{\min}$, and for simplicity I assume that the conductance in the nonresonant channel is trivially equal to $\frac{e^2}{h}$. For particles injected in the upper branch, the transmission is zero except near resonances corresponding to quasibound Dirac states. These resonances appear in the right region of the plateau, $E + \beta < U_0 < E_{\min}$, where the barrier is sufficiently high to produce negative energy states. For comparison, the QPC conductance calculated by explicit numerical integration of the Schrödinger equation corresponding to the Hamiltonian (3) is shown in Fig. 3(b). The analytical and numerical results are practically indistinguishable, except on the edges of the plateau. Note that, while I have taken a Gaussian barrier which smoothly decreases to zero in the asymptotic region, only the region near the top of the barrier, where it may be approximated by a harmonic potential $U(x) \approx U_0 - \frac{m\omega_x x^2}{2}$, is relevant to scattering. Numerics also indicated that different choices of barrier with the same curvature did not influence the result.

The lifetime of the rightmost resonance on the solid trace in Fig. 3 was calculated to be $\tau = 7.4 \times 10^{-10}$ s. The lifetime, according to (10) and (9), displays an exponential dependence on both α and β, which may be used to provide a highly sensitive and robust measurement of the Rashba coefficient. Upon increasing the magnetic field from 1 T to 3 T, the resonances become significantly narrower (Fig. 3). At 5 T, the lifetime is $\sim 10^{-8}$ s, and at 10 T, the lifetime is $\sim 10^{-1}$ s. In this limit an additional broadening of the resonance is expected at finite temperature due to inelastic electron-electron collisions in the channel; nevertheless our analysis shows that at high magnetic fields, the resonance is effectively bound. Note that while varying the magnetic field from 1 T to 3 T significantly narrows the resonant peaks, it does not change the number of resonances. This distinguishing behavior, which was derived earlier [see Eq. (12)] from the inverted harmonic oscillator spectrum (11), permits a straightforward identification of the effect in experiment.

Let us consider the spin structure of the bound state. At low values of η (i.e., $\beta \ll m\alpha^2$), the wave function inside the barrier is proportional to $\psi(x) \propto e^{i\int k dx}|+\rangle_y + e^{-i\int k dx}|-\rangle_y$, where $|\pm\rangle_y$ are spinors with polarization along the $\pm y$ axis. In such a state, both the current and magnetization are zero. Instead of a total spin, the state carries a total spin current $J_{x\mu}(x) = \frac{1}{2}\{v_x, s_\mu\}$ which is concentrated at the top of the barrier. The existence of a localized region of spin current is a consequence of the fact that, in the presence of a Zeeman gap, only states of one chirality participate in the tunneling process which leads to localization. In this sense the bound states considered here bear a strong similarity to chiral subgap (edge and surface) states in topological insulators [39], although they are supported by a smoothly varying potential rather than an edge. The current densities of the spin-up and spin-down components of the wave function are shown in Fig. 4(a) for the resonance corresponding to the $n = 1$ oscillator level at $gB_x = 4$ T.

It is straightforward to show that the localized spin current in our situation may be used to pump spin across the channel. Let us consider the spin states in the positive and negative energy bands $\epsilon_k^{\pm}$ near the anticrossing. In the positive energy branch, states with positive momenta have spin tilted towards the $-y$ axis, while states with negative momenta have spin tilted towards the $+y$ axis. In the negative energy branch,

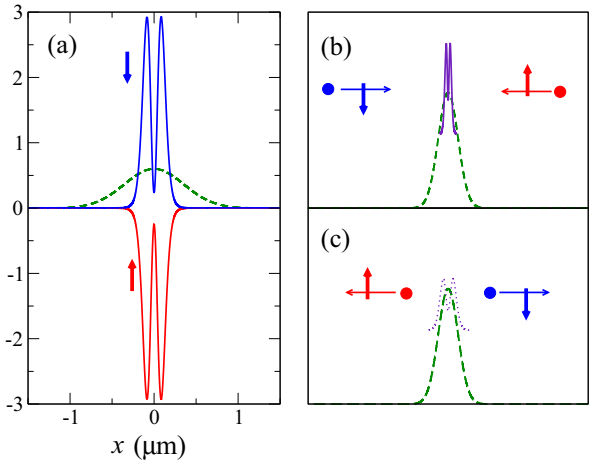

FIG. 4. (Color online) Spin current and spin pumping via the bound state. (a) The current densities (arb. units) in the spin-up and spin-down components of the wave function at resonance, $J_{x+} = \psi_+^* J_x \psi_+$ (red, positive curve) and $J_{x-} = \psi_-^* J_x \psi_-$ (blue, negative curve), where $\psi = \psi_+|+\rangle_y + \psi_-|-\rangle_y$. The barrier is shown by the dashed line. Since the state is localized, the total current everywhere is zero; however the state possesses a spin current $J_{xy} = \frac{J_{x+}-J_{x-}}{2}$. (b) Upon adiabatically switching on the magnetic field, a particle is captured inside the barrier from the left lead, initially in a spin-down state. (c) When the magnetic field is switched off instantaneously, the resonance decays, either returning the particle to the left lead in a spin-up state, or transferring it to the right lead in a spin-down state. The mirror process occurs for a particle injected from the right lead. This process increases the number of spin-up carriers in the left lead and the number of spin-down carriers in the right lead; i.e., it pumps spin across the channel in the absence of dc current.

the situation is opposite [see Fig. 1(a)]. Let us consider the component of spin current J_{xy} which is given by

$$J_{xy} = \frac{1}{4}\left\{\frac{p_x}{m} - \alpha\sigma_y, \sigma_y\right\} = \frac{p_x}{2m}\sigma_y - \frac{\alpha}{2}. \quad (14)$$

When $\alpha > 0$ the first term is negative for a positive energy state and positive for a negative energy state. Thus during the capture of a particle from the leads, the spin current of the particle is increased. In general, the bound state may be controlled by modulation of the parameters α, β which implies that the QPC can function as a spin transistor. We may perform, for example, a gedanken experiment in which the external magnetic field is first switched on slowly, resulting in the capture of a particle into the channel (assuming that the system is tuned so that the Fermi energy coincides with a resonance). During this process a positive energy state in the reservoirs is converted into a negative energy state in the constriction, and the spin current of the system is increased. Let us now instantaneously switch off the external magnetic field. Since the external field is required for trapping, the bound state decays and the particle is transferred into either the left or right reservoir. However, in the absence of the external magnetic field, the operator of spin current (14) commutes with the Hamiltonian (3). Thus the initial spin current generated by adiabatically switching on the magnetic field persists even in the absence of a localized state. It is straightforward to show that this process either transfers a particle from one reservoir to the other without changing its spin, or returns a particle to its original reservoir with a spin flip, as shown in Figs. 4(b) and 4(c). Cycling the applied field in this manner pumps spin from one reservoir to the other, generating a nonequilibrium polarization in the leads.

The level structure in the resonant regime is expected to be modified due to electron-electron interactions, which are most significant when only a few transverse channels are populated. Even in the lowest conductance ($\frac{e^2}{h}$) plateau, however, the Coulomb interaction remains strongly screened by carriers in the lower spin band (ϵ_k^-) which are freely transmitted above the barrier. Numerical calculations show that, in the Hartree approximation, the electron-electron interaction is well approximated by a contact interaction, and taking the random phase approximation the interaction takes the form

$$V(x-x') = \frac{2\pi\epsilon_r^{-1}e^2}{\left(1 - 2\pi e^2\epsilon_r^{-1}\Pi_{q\to 0,\omega=0}\right)}\delta(x-x'), \quad (15)$$

where ϵ_r is the permittivity, and in the first approximation we may take the static polarization operator for a uniform 1D channel, $\Pi_{q\to 0,\omega=0} = -\frac{1}{2\pi v_F}$, where $v_F = \sqrt{2mE_F}$ is the Fermi velocity. The charging energy is $\approx \frac{2\pi v_F}{2a}$ where $2a$ is the size of the bound states. In the harmonic approximation, we have $a = \sqrt{2m\omega^*(n+\frac{1}{2})}$ for the nth oscillator level, which is typically of the order of the barrier width for the lowest bound state, $a \approx l = \sqrt{\frac{8U_0}{m\omega_x^2}}$; this shows that it is possible to tune the charging energy to a low fraction of the Fermi energy by making the barrier sufficiently smooth. Taking typical parameters for a GaAs hole QPC, the charging energy for the lowest occupied ($n = 3$) state is $\approx$0.1 meV.

The presence of one or more bound states in the channel may be accounted for by an effective potential, $U_{\rm eff} = U(x) + U_H(x)$, where the Hartree potential is

$$U_H(x) = \int V(x-x')|\psi(x')|^2 dx. \quad (16)$$

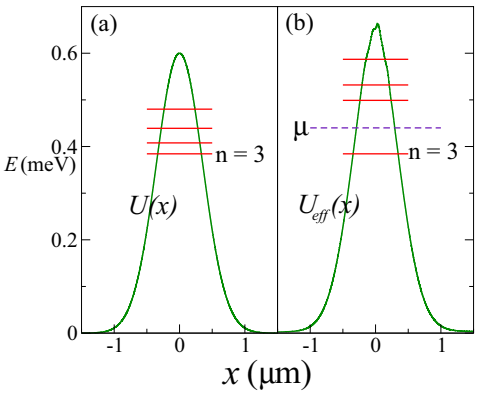

FIG. 5. (Color online) The resonant spectrum calculated in the Hartree approximation with $N = 0$ (a) and $N = 1$ (b) particles captured in the channel. The barrier $U(x)$ and effective potential $U_{\rm eff}(x)$ which account for the Hartree potential are shown in the background. The resonant energies are indicated by solid horizontal lines, and the chemical potential μ is shown by dashed horizontal lines.

The Hartree potential alters both the height $U_{\text{eff}}(0)$ and the shape of the barrier. The increased barrier height yields a positive shift in the energy of multiparticle bound states; however since the number of bound states (11) depends only on the level spacing and not on the barrier height, this does not reduce the number of states. At the same time, the number of states may be affected by a change in the shape of the barrier. In the typical situation, the lowest occupied state in the channel is an oscillator state with index $n > 0$; the corresponding probability density $|\psi(x)|^2$ and Hartree potential $U_H(x)$ are oscillating at the top of the barrier, rather than sharply peaked. Numerical calculations show that the level spacing is not significantly affected, although it may be slightly reduced due to the flattening of the barrier due to the Hartree contribution, increasing the number of resonances. The effective potential and spectrum in the presence of a single occupied state are shown in Fig. 5 for the same parameters used in Fig. 3.

These results illustrate that the transmission problem is highly nontrivial in a 1D system with Rashba interaction even in the absence of interactions or multichannel effects. The conductance on the Zeeman plateaus, $G = (n + \frac{1}{2})\frac{2e^2}{h}$, is characterized by resonances associated with confinement in a single spin channel, and this effect generally occurs in systems with smoothly varying repulsive potential and a magnetic field applied in a particular orientation. Furthermore, these results illustrate a surprising manifestation of Dirac physics in ballistic 1D channels, which is clearly indicated by the presence of Schwinger pair production, yielding antifermion states which exhibit properties highly suitable for applications in spintronics. In contrast to the situation in both high-energy physics and other emergent Dirac systems such as graphene and the topological insulators, the parameters controlling the Dirac equation are tunable in our situation: the magnetic field is analogous to the Dirac mass, the spin-orbit interaction to the speed of light, and the electric field is provided by the smooth 1D potential inside the constriction. The similarity and tunability of these energy scales allows for remarkable control over the properties of the Dirac states and enhances the versatility of the system for applications to spintronics.

This work was partially supported by the Australian Research Council (DP120101859). The author wishes to acknowledge O. P. Sushkov, J. Ingham, G. Vionnet, M. Veldhorst, I. S. Terekhov, and A. R. Hamilton for valuable discussions.

[1] R. M. Lutchyn, J. D. Sau, and S. Das Sarma, Phys. Rev. Lett. **105**, 077001 (2010).
[2] Y. Oreg, G. Refael, and F. von Oppen, Phys. Rev. Lett. **105**, 177002 (2010).
[3] V. Mourik, K. Zuo, S. M. Frolov, S. R. Plissard, E. P. A. M. Bakkers, and L. P. Kouwenhoven, Science **336**, 6084 (2012).
[4] F. Mireles and G. Kirczenow, Phys. Rev. B **64**, 024426 (2001).
[5] M. Governale and U. Zülicke, Phys. Rev. B **66**, 073311 (2002).
[6] B. Wang, J. Wang, and H. Guo, Phys. Rev. B **67**, 092408 (2003).
[7] J.-F. Liu, K. S. Chan, and Jun Wang, Appl. Phys. Lett. **101**, 082407 (2012).
[8] G. Liu and G. Zhou, J. Appl. Phys. **101**, 063704 (2007).
[9] F. Xi and Z. Guang-Hi, Commun. Theor. Phys. **51**, 341 (2009).
[10] A. V. Moroz and C. H. W. Barnes, Phys. Rev. B **60**, 14272 (1999).
[11] Y. V. Pershin, J. A. Nesteroff, and V. Privman, Phys. Rev. B **69**, 121306 (2004).
[12] G. Usaj and C. A. Balseiro, Phys. Rev. B **70**, 041301(R) (2004).
[13] S. Chesi, G. F. Giuliani, L. P. Rokhinson, L. N. Pfeiffer, and K. W. West, Phys. Rev. Lett. **106**, 236601 (2011).
[14] T. Li and O. P. Sushkov, Phys. Rev. B **87**, 165434 (2013).
[15] M.-H. Liu, C.-R. Chang, and S.-H. Chen, Phys. Rev. B **71**, 153305 (2005).
[16] D. Sánchez and L. Serra, Phys. Rev. B **74**, 153313 (2006).
[17] X. B. Xiao and Y. G. Chen, Europhys. Lett. **90**, 47004 (2010).
[18] X. B. Xiao, F. Li, Y. G. Chen, and N. H. Liu, Eur. Phys. J. B **85**, 112 (2012).
[19] J. Schwinger, Phys. Rev. **82**, 664 (1951).
[20] S. V. Bulanov, T. Esirkepov, and T. Tajima, Phys. Rev. Lett. **91**, 085001 (2003).
[21] R. Ruffini, G. Vereshchagin, and S.-S. Xue, Phys. Rep. **487**, 1 (2010).
[22] D. Allor, T. D. Cohen, and D. A. McGady, Phys. Rev. D **78**, 096009 (2008).
[23] M. Lewkowicz and B. Rosenstein, Phys. Rev. Lett. **102**, 106802 (2009).
[24] M. Büttiker, Phys. Rev. B **41**, 7906(R) (1990).
[25] G. Engels, J. Lange, T. Schäpers, and H. Lüth, Phys. Rev. B **55**, R1958 (1997).
[26] J. Luo, H. Munekata, F. F. Fang, and P. J. Stiles, Phys. Rev. B **41**, 7685 (1990).
[27] D. Grundler, Phys. Rev. Lett. **84**, 6074 (2000).
[28] Y. A. Bychkov and E. I. Rashba, JETP Lett. **39**, 78 (1984).
[29] B. Grbic, R. Leturcq, T. Ihn, K. Ensslin, D. Reuter, and A. D. Wieck, Phys. Rev. B **77**, 125312 (2008).
[30] F. Nichele, A. N. Pal, R. Winkler, C. Gerl, W. Wegscheider, T. Ihn, and K. Ensslin, Phys. Rev. B **89**, 081306(R) (2014).
[31] R. Winkler, *Spin-Orbit Coupling Effects in Two-Dimensional Electron and Hole Systems*, Springer Tracts in Modern Physics Vol. 191 (Springer, Berlin, 2003).
[32] N. K. Patel, J. T. Nicholls, L. Martin-Moreno, M. Pepper, J. E. F. Frost, D. A. Ritchie, and G. A. C. Jones, Phys. Rev. B **44**, 13549 (1991).
[33] D. L. Burke *et al.*, Phys. Rev. Lett. **79**, 1626 (1997).
[34] Y. Wang *et al.*, Science **340**, 734 (2013).
[35] O. Klein, Z. Phys. **53**, 157 (1929).
[36] M. I. Katnelson, K. S. Novoselov, and A. K. Geim, Nature (London) **2**, 620 (2006).
[37] Z. Q. Yuan, R. R. Du, M. J. Manfra, L. N. Pfeiffer, and K. W. West, Appl. Phys. Lett. **94**, 052103 (2009).
[38] J. C. H. Chen *et al.*, New J. Phys. **12**, 033043 (2010).
[39] M. Wada, S. Murakami, F. Freimuth, and G. Bihlmayer, Phys. Rev. B **83**, 121310(R) (2011).